

# Chemical Science

Accepted Manuscript



This is an *Accepted Manuscript*, which has been through the Royal Society of Chemistry peer review process and has been accepted for publication.

*Accepted Manuscripts* are published online shortly after acceptance, before technical editing, formatting and proof reading. Using this free service, authors can make their results available to the community, in citable form, before we publish the edited article. We will replace this *Accepted Manuscript* with the edited and formatted *Advance Article* as soon as it is available.

You can find more information about *Accepted Manuscripts* in the [Information for Authors](#).

Please note that technical editing may introduce minor changes to the text and/or graphics, which may alter content. The journal's standard [Terms & Conditions](#) and the [Ethical guidelines](#) still apply. In no event shall the Royal Society of Chemistry be held responsible for any errors or omissions in this *Accepted Manuscript* or any consequences arising from the use of any information it contains.



Journal Name

ARTICLE

## Stimuli-responsive colorimetric and NIR fluorescence combination probe for selective reporting of cellular hydrogen peroxide

Nagarjun Narayanaswamy,<sup>a</sup> Sivakrishna Narra,<sup>b</sup> Raji R. Nair,<sup>c</sup> Deepak Kumar Saini,<sup>c</sup> Paturu Kondaiah<sup>b</sup> and T. Govindaraju<sup>\*a</sup>

Received 00th January 20xx,  
Accepted 00th January 20xx

DOI: 10.1039/x0xx00000x

www.rsc.org/

Hydrogen peroxide (H<sub>2</sub>O<sub>2</sub>) is a key reactive oxygen species and a messenger in cellular signal transduction apart from playing a vital role in many biological processes in living organisms. In this Article, we present phenyl boronic acid-functionalized quinone-cyanine (**QCy-BA**) in combination with AT-rich DNA (exogenous or endogenous cellular DNA), *i.e.*, **QCy-BA**∩DNA as a stimuli-responsive NIR fluorescence probe for *in vitro* levels of H<sub>2</sub>O<sub>2</sub>. In response to cellular H<sub>2</sub>O<sub>2</sub> stimulus, **QCy-BA** converts into **QCy-DT**, a one-donor-two-acceptor (D2A) system that exhibits switch-on NIR fluorescence upon binding to the DNA minor groove. Fluorescence studies on the combination probe **QCy-BA**∩DNA showed strong NIR fluorescence selectively in the presence of H<sub>2</sub>O<sub>2</sub>. Further, glucose oxidase (GOx) assay confirmed the high efficiency of the combination probe **QCy-BA**∩DNA for probing H<sub>2</sub>O<sub>2</sub> generated *in situ* through GOx-mediated glucose oxidation. Quantitative analysis through fluorescence plate reader, flow cytometry and live imaging approaches showed that **QCy-BA** is a promising probe to detect the normal as well as elevated levels of H<sub>2</sub>O<sub>2</sub> produced by EGF/Nox pathways and post-genotoxic stress in both primary and senescent cells. Overall, **QCy-BA**, in combination with exogenous or cellular DNA, is a versatile probe to quantify and image H<sub>2</sub>O<sub>2</sub> in normal and disease-associated cells.

### Introduction

The regulation of redox homeostasis is essential for maintaining normal cellular functions such as signaling, growth, survival, and death.<sup>1</sup> Anomalous behavior of redox homeostasis adversely affects the normal physiological functions and in turn, responsible for numerous pathological conditions.<sup>1</sup> Normally, cells in the disease state exhibit high levels of aerobic glycolysis (Warburg effect), which results in oxidative stress.<sup>2</sup> For example, the oxidative stress in cancer cells results in the accumulation of high levels of reactive oxygen species (ROS).<sup>3</sup> ROS constitute an important class of chemically reactive species that are essential for normal cellular functions including cell proliferation and differentiation.<sup>4</sup> The optimum levels of ROS are controlled by various cellular redox homeostasis mechanisms, and an abrupt increase in their concentration levels is directly linked to oxidative stress-related disorders. Abnormally high levels of ROS are generated in response to adverse environmental and physiological stresses, exposure to ultraviolet (UV) light, and ionizing and heat radiations.<sup>3c</sup> It is crucial to monitor the levels of intracellular ROS for maintaining effective cellular

homeostasis. Notably, different levels of ROS are responsible for different biological responses.<sup>5</sup> The cell maintains different levels of ROS by activating the ROS-scavenging systems such as superoxide dismutases, glutathione peroxidase, redox enzymes (peroxiredoxins, glutaredoxin, and thioredoxin) and catalase. Misregulation in any of these ROS-scavenging processes leads to the generation of excess amounts of ROS. Accumulation of high levels of ROS causes oxidative damage to cellular components such as proteins, lipids and nucleic acids, which is responsible for aging and many pathological conditions including cancer, cardiovascular, inflammatory and neurodegenerative diseases.<sup>6,7</sup> It is known that cellular aging, also called cellular senescence, is a permanent cell cycle arrest state that results in increased production of ROS species.<sup>7a</sup> This increased ROS production is critical to maintaining the viability of the senescent cell.<sup>7b</sup> Therefore, it is necessary to develop molecular tools that are highly sensitive and can be activated by high levels of ROS to distinguish aged or disease-associated cells from normal cells.

ROS mainly comprises free radicals such as hydroxyl radical (OH·) and superoxide (O<sub>2</sub><sup>·-</sup>), and reactive molecular species such as H<sub>2</sub>O<sub>2</sub>. H<sub>2</sub>O<sub>2</sub> is one of the most prominent and essential ROS in biological systems, and its significantly higher levels are generated in aged and cancer cells than in normal cells.<sup>8</sup> In fact, H<sub>2</sub>O<sub>2</sub> is a small molecular metabolite and plays a vital role in the regulation of various physiological processes in living organisms.<sup>9</sup> Most importantly, H<sub>2</sub>O<sub>2</sub> serves as a messenger in normal cellular signal transduction and is also a known marker for oxidative damage in many disease-

<sup>a</sup>Bioorganic Chemistry Laboratory, New Chemistry Unit, Jawaharlal Nehru Centre for Advanced Scientific Research, Jakkur P.O., Bengaluru 560064, India.

<sup>b,c</sup>Department of Molecular Reproduction, Development and Genetics, Indian Institute of Science, Bengaluru 560 012, India.

<sup>†</sup>Electronic Supplementary Information (ESI) available: Synthesis, characterization, UV-vis absorption, emission, catalase assay, cell viability and FACS data. See DOI: 10.1039/x0xx00000x

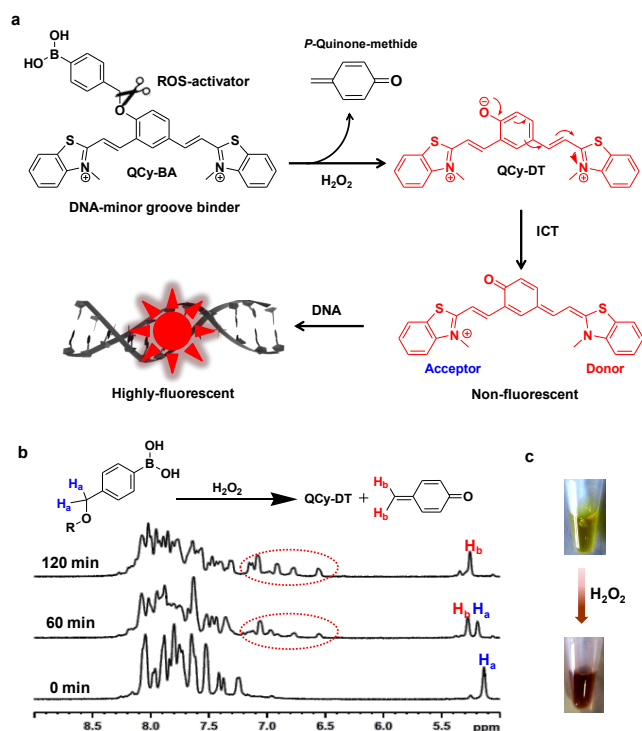


**Fig. 1** (a) Schematic representation of conversion of **QCy-BA** to *p*-quinone-methide and **QCy-DT**, a DNA minor groove binder, in the presence of  $\text{H}_2\text{O}_2$ . (b) Time-dependent  $^1\text{H}$  NMR spectral monitoring of slicing of phenyl boronic acid of **QCy-BA** in the presence of  $\text{H}_2\text{O}_2$ . Red circles highlight the appearance of new signals for the newly-formed quinone system and **QCy-DT**.  $\text{H}_a$  and  $\text{H}_b$  represent the  $\text{O}-\text{CH}_2$  ( $\text{C}-\text{H}_a$ ) bearing phenyl boronic acid group and newly-formed exocyclic ( $\text{C}-\text{H}_b$ ) protons of *p*-quinone-methide, respectively. (c) The change in solution color upon addition of  $\text{H}_2\text{O}_2$  to **QCy-BA**, as visualized after 2h.

associated cells.<sup>9</sup> In cells,  $\text{H}_2\text{O}_2$  is generated through the tyrosine kinase receptor-mediated NADPH oxidase (Nox) activation, which affects the functioning of signaling proteins that control cell signaling, proliferation, senescence, and death.<sup>10</sup> The biological significance of  $\text{H}_2\text{O}_2$  in human physiology and pathology has generated immense interest in understanding the mechanistic details of its generation, partition and role in cellular function and signaling pathways. In comparison to other ROS, relatively higher stability and diffusion rates of  $\text{H}_2\text{O}_2$  through the plasma membrane makes it an attractive candidate to study its signaling pathways in living cells.<sup>10</sup> However, studies in the spatiotemporal dynamics of  $\text{H}_2\text{O}_2$  as a messenger in cellular signal transduction have been limited on account of its chemical reactivity and instability. Molecular imaging of  $\text{H}_2\text{O}_2$  using fluorescence probes is a highly attractive tool for studying its generation, accumulation,<sup>11</sup> trafficking, and role in biological processes in a spatiotemporal manner in living cells.<sup>12</sup> Recently, a new class of organochalcogens such as selenium and tellurium-based fluorescence redox probes have been developed and explored for the *in vivo* imaging and real-time monitoring of ROS in cells.<sup>13</sup>

In recent years, stimuli-responsive fluorescence probes are gaining momentum due to their flexibility in introducing diversity through chemical modification and liberation of biologically active probes at the site of target cellular organelles, in response to biological analytes of interest.<sup>14</sup>

Moreover, targeting specific subcellular organelles (mitochondria) and biomolecules such as DNA and proteins using stimuli-responsive fluorescence probes is an emerging and powerful imaging technique that presents enormous potential in biomedical applications related to diagnostics and therapeutics.<sup>15</sup> In this context, we envisaged the functionalization of a DNA-binding fluorescence dye with a stimuli-responsive appendage as a promising and unconventional but efficient method of *in situ* generation of an active probe in response to  $\text{H}_2\text{O}_2$ . Our group has been actively involved in the development of novel red fluorescence probes for biologically relevant thiols, metal ions and nucleic acids.<sup>16</sup> Recently, we have developed a sequence-specific DNA minor groove probe **QCy-DT**, which shows switch-on NIR fluorescence specifically in the presence of AT-rich DNA (exogenous or endogenous cellular DNA).<sup>17</sup> Structurally, **QCy-DT** has a free hydroxyl group readily available for functionalization with a large number of chemically or enzymatically cleavable appendages to make it a versatile and promising stimuli-responsive probe. In response to a specific stimulus (chemical or enzyme), the appendage functionality is cleaved to release an NIR fluorescence-ready **QCy-DT** probe, which upon binding the minor groove of DNA fluoresces strongly, thus, aiding the imaging and quantification of the stimulus. We anticipated that functionalizing the DNA binding fluorescence probe **QCy-DT** with aryl boronates would be an attractive strategy for the development of a stimuli-responsive fluorescence probe for  $\text{H}_2\text{O}_2$ , as it provides sensitivity and built-in-correction to the probe against background signals from the cellular environment. Therefore, **QCy-DT** hydroxyl group was functionalized to obtain phenyl boronic acid-conjugated quinone-cyanine (**QCy-BA**, Fig. 1a), which reacts selectively with  $\text{H}_2\text{O}_2$  to release the parent DNA binding dye. We selected phenyl boronate as the preferred appendage owing to the fact that the reaction between  $\text{H}_2\text{O}_2$  and boronic acid or ester is highly chemospecific, bioorthogonal and biocompatible while the byproducts are non-toxic to living cells.<sup>11,18,19</sup> Thus, we envision that probe **QCy-BA**, in combination with exogenous or endogenous cellular DNA, will be a promising, stimuli-responsive fluorescence probe for investigating  $\text{H}_2\text{O}_2$  production and concentration levels in living cells, which will further facilitate the imaging and diagnosis of disease-associated cells.

## Results and discussion

**Synthesis and design principle of  $\text{H}_2\text{O}_2$ -triggered release of DNA minor groove binder.** Aryl boronates are unique chemical moieties with selective reactivity towards the ambiphilic  $\text{H}_2\text{O}_2$ , a desirable property to achieve specificity and selectivity over other biologically relevant ROS.<sup>11</sup> Initially, the boronate functionality acts as an electrophilic center and reacts with the nucleophile to generate the tetrahedral-boronate complex.<sup>11e</sup> Subsequently, the carbon-boron (C-B) bond becomes labile and acts as a nucleophile towards the electrophilic oxygen center of  $\text{H}_2\text{O}_2$ . In particular, the aryl boronate functionality becomes a specific reorganization center for  $\text{H}_2\text{O}_2$  among all

other biological oxygen metabolites and ROS, which operates through one electron transfer or electrophilic oxidation pathways.<sup>11</sup>

Herein, we present a stimuli-responsive probe **QCy-BA**, a DNA minor groove binder (**QCy-DT**) functionalized with phenyl boronic acid. Although **QCy-BA** shares the backbone of Cy7 dyes, the major structural difference comes from two positively charged, nitrogen atom-containing benzothiazoles with distinct conjugation patterns around the central phenolic moiety derivatized with phenyl boronic acid functionality.<sup>17,20</sup> Furthermore, the electron delocalization in **QCy-BA** is disrupted as a consequence of masking the central phenolic hydroxyl with phenyl boronic acid functionality. Upon slicing of the phenyl boronic acid functionality, in response to the H<sub>2</sub>O<sub>2</sub> stimulus, **QCy-BA** transforms into the negatively charged phenolate of **QCy-DT**. The generation of phenolate restores the electron transfer towards one of the positively charged nitrogen atoms of the benzothiazole acceptor. This restores internal charge transfer (ICT) to generate a highly electron delocalized  $\pi$ -system similar to Cy-7 dye with NIR-fluorescence in the presence of DNA (as shown in Fig. 1a).<sup>17</sup>

Synthesis of **QCy-BA** was achieved by treating 4-(hydroxymethyl)phenyl boronic acid with a pinacol in the presence of magnesium sulfate in acetonitrile to obtain 4-(hydroxymethyl)phenyl boronic ester (**1**) (ESI Scheme 1). The phenyl boronic ester **1** was treated with NaI and trimethyl silyl chloride in acetonitrile at 0 °C to give 4-(iodomethyl)phenyl boronic ester (**2**).<sup>20a</sup> The 4-(iodomethyl)phenyl boronic ester (**2**) was coupled to 4-hydroxy isophthalaldehyde using potassium carbonate as a base in dimethylformamide (DMF) at room temperature to obtain phenyl boronic ester dialdehyde (**3**) in good yield. Finally, the dialdehyde (**3**) was coupled with *N*-methylated benzothiazole in the presence of piperidine to yield the probe **QCy-BA**. All the intermediates and probe **QCy-BA** were characterized by NMR and high-resolution mass spectroscopy (HRMS).

**NMR-analysis of H<sub>2</sub>O<sub>2</sub>-triggered release of DNA minor groove binder.** In a preliminary study, we carried out time-dependent NMR spectroscopy analysis of **QCy-BA** in the presence of H<sub>2</sub>O<sub>2</sub> to assess the stimuli-responsive slicing of phenyl boronic acid functionality. The <sup>1</sup>H NMR spectrum of **QCy-BA** (2 mM) alone in D<sub>2</sub>O (0.5 mL) showed a single peak at 5.10 ppm corresponding to the O-CH<sub>2</sub> (C-H<sub>a</sub>)-bearing phenyl boronic acid group and peaks at 8.2-7.2 ppm corresponding to aromatic protons of the parent **QCy-DT**. The chemical shifts of O-CH<sub>2</sub>, aromatic region of **QCy-BA** and appearance of possible new peaks for *p*-quinone methide (sliced byproduct corresponding to phenyl boronic acid functionality) upon sequential addition of H<sub>2</sub>O<sub>2</sub> was monitored. After 1 h of H<sub>2</sub>O<sub>2</sub> (10 mM, 5  $\mu$ L from the stock H<sub>2</sub>O<sub>2</sub> of 1M) addition, the peak intensity at 5.10 ppm, *i.e.*, C-H<sub>a</sub> (O-CH<sub>2</sub>) gradually decreased and new peaks appeared at 5.20 ppm and 6.5-7.0 ppm regions, suggesting the coexistence of both phenyl boronic acid protected and deprotected forms of **QCy-BA**. The peaks at 5.20 ppm and aromatic region 6.5-7.0 ppm corresponds to the newly-formed exocyclic C-H<sub>b</sub> protons of *p*-quinone-methide and **QCy-DT**

moieties, respectively. After 2 h, we observed a single peak at 5.20 ppm and prominent new peaks at 6.5-7.0 ppm, indicating the complete conversion of **QCy-BA** to **QCy-DT** and *p*-quinone methide (Fig. 1b). This study confirmed the H<sub>2</sub>O<sub>2</sub> stimulus-triggered slicing of phenyl boronic acid functionality of **QCy-BA** to release **QCy-DT**, a DNA minor groove binding probe. Interestingly, the color of the solution changed from yellow to brown after the addition of H<sub>2</sub>O<sub>2</sub> to **QCy-BA**, a naked eye detection of the formation of *p*-quinone-methide and **QCy-DT** (Fig. 1c).

#### Photophysical properties of **QCy-BA** in the presence of H<sub>2</sub>O<sub>2</sub>.

Next, we studied the photophysical properties of **QCy-BA** in the absence and presence of H<sub>2</sub>O<sub>2</sub> using UV-vis absorption and emission studies in PBS-buffer solution (10 mM, pH = 7.4) under ambient conditions. UV-vis absorption spectrum of **QCy-BA** (5  $\mu$ M) showed broad absorbance in the 300-500 nm region with an absorption maximum ( $\lambda_{\max}$ ) at 400 nm. Upon excitation at 400 nm, the emission spectrum of **QCy-BA** (5  $\mu$ M) showed weak fluorescence with emission maximum ( $E_{\max}$ ) at 565 nm (Fig. S1b). As expected, **QCy-BA** did not emit in the NIR region due to phenyl boronic acid protection of the backbone-phenolic hydroxyl moiety. Interestingly, absorption spectrum of **QCy-BA** (5  $\mu$ M) showed a gradual decrease in absorption maxima at 400 nm in the presence of H<sub>2</sub>O<sub>2</sub> (1 mM); this was accompanied by the appearance of a new absorption band at 465 nm with a shoulder at 530 nm and an isosbestic point at 442 nm (Fig. S1a). The new absorption bands at 465 nm and 530 nm revealed the transformation of **QCy-BA** to the phenolate form of **QCy-DT**. In agreement with the NMR study (Fig. 1b), UV-vis absorption data confirmed the generation of **QCy-DT** through H<sub>2</sub>O<sub>2</sub>-assisted oxidation of boronic acid in **QCy-BA** followed by the hydrolysis and 1,6-elimination of *p*-quinone-methide group (Fig. S2).<sup>11e,20a</sup> Evidently, UV-vis absorption spectral characteristics clearly support the observed change in solution color from yellow to brown, as a result of the newly formed **QCy-DT** ( $\lambda_{\max}$  at 465 and 530 nm) from **QCy-BA** ( $\lambda_{\max}$  = 400 nm) (Fig. 1c). The emission spectra of **QCy-BA** (5  $\mu$ M) in the presence of H<sub>2</sub>O<sub>2</sub> (1 mM) displayed a gradual decrease in fluorescence intensity at 565 nm and a weak basal level fluorescence band centered around 680 nm, with a large Stokes shift ( $\Delta\lambda_{\max}$  = ~280 nm) upon excitation at 400 nm (Fig. S1b). Therefore, H<sub>2</sub>O<sub>2</sub>-triggered slicing of phenyl boronic acid functionality of **QCy-BA** is a highly useful transformation for the generation of stimuli-responsive

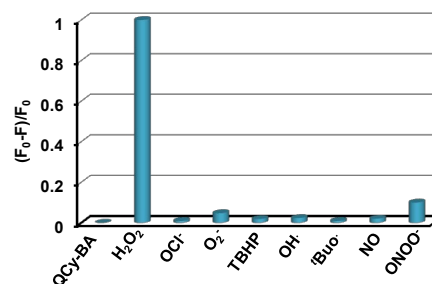


Fig. 2 Fluorescence response of **QCy-BA** (5  $\mu$ M) to various reactive oxygen species (ROS) at an individual concentration of 100  $\mu$ M. Where, F<sub>0</sub> and F are the fluorescence intensities of **QCy-BA** in absence and presence of ROS respectively.

switch-on DNA binding fluorescence probe **QCy-DT** owing to its large Stokes shift and non-fluorescence in the unbound state.

Further, we performed concentration-dependent fluorescence study on slicing of the phenyl boronic acid functionality of **QCy-BA** (5  $\mu\text{M}$ ) in response to the sequential addition of  $\text{H}_2\text{O}_2$  (5 to 100  $\mu\text{M}$ ). The fluorescence intensity of **QCy-BA** at 565 nm was decreased in response to added  $\text{H}_2\text{O}_2$  in the concentration range of 5 to 50  $\mu\text{M}$  and subsequently reached saturation at 100  $\mu\text{M}$ . A linear relationship ( $R^2 = 0.9877$ ) was observed with increasing concentration of  $\text{H}_2\text{O}_2$  in the concentration range of 5–20  $\mu\text{M}$ . Based on  $3\sigma/\text{slope}$ , the limit of detection (LOD) of  $\text{H}_2\text{O}_2$  was found to be 5.3  $\mu\text{M}$ , using the decrease in fluorescence of **QCy-BA** at 565 nm (Fig. S3).<sup>21</sup>

$\text{H}_2\text{O}_2$  is one of the many ROS present in the biological systems, and it is necessary to test the probe **QCy-BA** against all of them to assess its selectivity and specificity. Therefore, we examined the response of **QCy-BA** towards  $\text{H}_2\text{O}_2$  (100  $\mu\text{M}$ ) in the presence of other ROS (100  $\mu\text{M}$ ), including tertbutylhydroperoxide (TBHP), superoxide ( $\text{O}_2^-$ ), hydroxyl radical ( $\text{HO}\cdot$ ), tert-butoxy radical ( $^t\text{BuO}\cdot$ ), hypochlorite ( $\text{OCl}^-$ ) peroxyxynitrite ( $\text{ONOO}^-$ ) and nitric oxide (NO). Remarkably, only  $\text{H}_2\text{O}_2$  efficiently decreased the fluorescence emission at 565 nm owing to selective slicing of phenyl boronic acid functionality of the **QCy-BA** (5  $\mu\text{M}$ ). On the other hand, we observed very minimal or no effect on the probe response in the presence of  $\text{O}_2^-$ ,  $\text{HO}\cdot$ ,  $^t\text{BuO}\cdot$ ,  $\text{OCl}^-$ ,  $\text{ONOO}^-$  and NO (Fig. 2). These results are in agreement with the selective 1,6-elimination of phenyl boronic acid functionality of **QCy-BA** only in the presence of  $\text{H}_2\text{O}_2$  to liberate the *p*-quinone-methide moiety and **QCy-DT**.<sup>19,20</sup>

**Photophysical properties of combination probe QCy-BACDrew-AT in the presence of  $\text{H}_2\text{O}_2$ .** To further validate the  $\text{H}_2\text{O}_2$ -stimulated conversion of **QCy-BA** to **QCy-DT**, a DNA minor groove binder, the transformation was monitored using UV-vis absorption and emission studies in the presence of an AT-rich DNA strand (Drew-AT: 5'-GCGCAAATTTGCGC-3'). **QCy-DT** binds AT-rich DNA minor groove with high sequence-specificity (5'-AAATTT-3'), which reflects in the strong NIR-fluorescence.<sup>17</sup> Thus, we chose Drew-AT, a self-complementary 14-base pair (bp) sequence containing central 5'-AAATTT-3' sequence<sup>22</sup> for fluorescence reporting of **QCy-DT** released in response to  $\text{H}_2\text{O}_2$  stimulus, by means of strong emission in the NIR region. The absorption spectrum of **QCy-BA** (2  $\mu\text{M}$ ), in the presence of Drew-AT (2  $\mu\text{M}$ ) duplex, showed an increase in absorption maxima at 416 nm with bathochromic shift ( $\Delta\lambda_{\text{max}} = 16$  nm) (Fig. S4a). On the other hand, the fluorescence spectrum of **QCy-BA** (2  $\mu\text{M}$ ), in the presence of Drew-AT, showed emission maxima at 500 nm with hypsochromic shift ( $\Delta\lambda_{\text{max}} = \sim 50$  nm) (Fig. S4b). These changes in absorption and emission spectra are attributed to weak interactions between **QCy-BA** and Drew-AT duplex through electrostatic and hydrophobic interactions. Next, absorption and emission spectra of **QCy-BA** were recorded in the presence of Drew-AT duplex and  $\text{H}_2\text{O}_2$  (100  $\mu\text{M}$ ). The absorption spectrum showed a gradual decrease in absorption

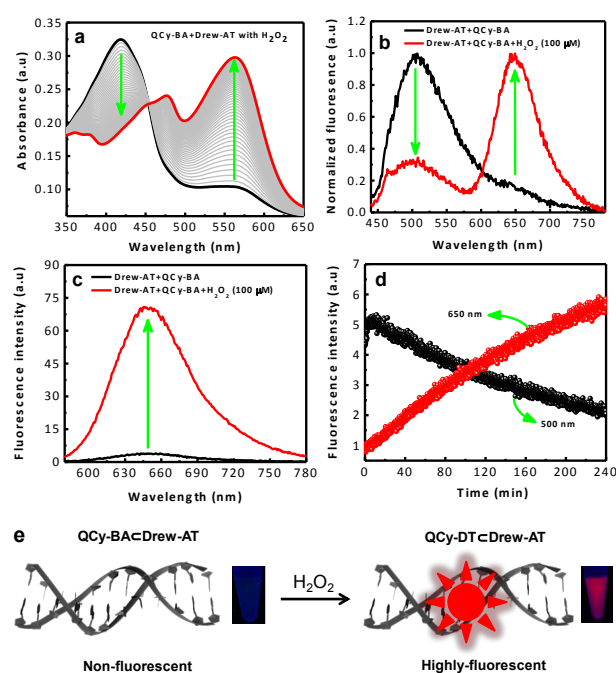


**Fig. 3** (a) Absorption spectra of combination probe **QCy-BACDrew-AT** (2  $\mu\text{M}$ ) in the presence of  $\text{H}_2\text{O}_2$  (100  $\mu\text{M}$ ) in PBS-buffer solution as a function of time. (b) Normalized fluorescence spectra of **QCy-BA** (2  $\mu\text{M}$ ) in the presence of Drew-AT (2  $\mu\text{M}$ ) upon excitation at 400 nm. (c) Fluorescence spectra of **QCy-BA** (2  $\mu\text{M}$ ) in the presence of Drew-AT (2  $\mu\text{M}$ ) upon excitation at 564 nm. All the spectra are acquired in the presence of  $\text{H}_2\text{O}_2$  (100  $\mu\text{M}$ ). (d) Time-dependent fluorescence spectra of **QCy-BA** (2  $\mu\text{M}$ ) in the presence of Drew-AT (2  $\mu\text{M}$ ) after the addition of  $\text{H}_2\text{O}_2$  (100  $\mu\text{M}$ ) upon excitation at 400 nm. (e) Schematic view of conversion of **QCy-BA** to *p*-quinone-methide and a DNA minor groove binder (**QCy-DT**) with turn-on NIR fluorescence, in the presence of  $\text{H}_2\text{O}_2$ .

at 416 nm with corresponding increase in the absorption at 564 nm with an isosbestic point at 456 nm, which is in agreement with the absorption characteristics observed for **QCy-DT/Drew-AT** complex (Fig. 3a).<sup>17</sup> Similarly, the emission spectrum of **QCy-BA** (excitation at  $\lambda_{\text{max}} = 400$  nm), in the presence of Drew-AT duplex and  $\text{H}_2\text{O}_2$ , showed fluorescence decrease at 500 nm and a corresponding increase at 650 nm (Fig. 3b). This remarkable ratiometric emission at 500 nm and 650 nm ( $\Delta\lambda_{\text{max}} = \sim 250$  nm) is a desirable property of a fluorescence probe in increasing signal-to-noise ratio; measurement at low wavelengths minimizes the error arising from various environmental factors. Upon excitation with wavelength corresponding to the isosbestic point (456 nm), probe **QCy-BA** in combination with Drew-AT showed gradual increase in  $I_{650}/I_{500}$  ratio as function of time (0 to 80 min) and concentration of  $\text{H}_2\text{O}_2$  (0 to 200  $\mu\text{M}$ ) (Fig. S5). Further, upon excitation at 564 nm ( $\lambda_{\text{max}}$  of **QCy-DT** bound to Drew-AT duplex), strong fluorescence enhancement at 650 nm was observed (Fig. 3c). Furthermore, probe **QCy-BA** in combination with Drew-AT showed selective fluorescence enhancement at 650 nm in presence  $\text{H}_2\text{O}_2$  over other ROS (Fig. S6). These results, reiterated that the  $\text{H}_2\text{O}_2$ -triggered conversion of **QCy-BA** to a DNA minor groove binder **QCy-DT** is a promising ratiometric fluorescence platform for  $\text{H}_2\text{O}_2$  in the presence of exogenous DNA (Drew-AT).

The time-dependent, fluorescence study was carried out to evaluate the release kinetics of **QCy-BA** (2  $\mu\text{M}$ ) to **QCy-**

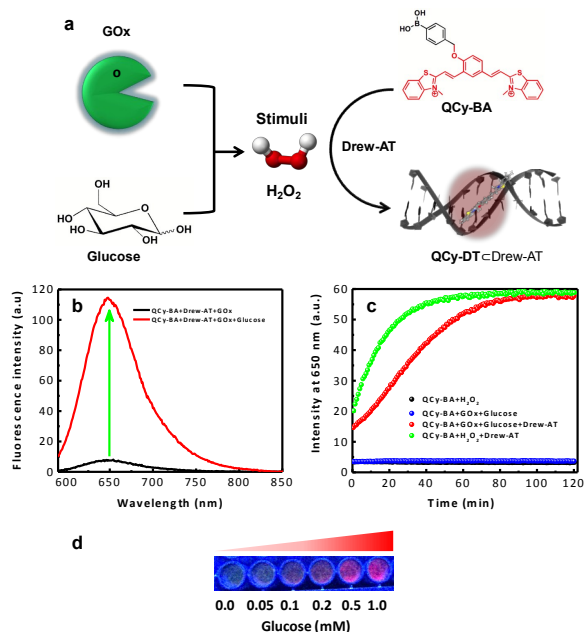


**Fig. 4** (a) Schematic diagram showing the GOx-assay where GOx oxidizes glucose to gluconic acid, generating H<sub>2</sub>O<sub>2</sub>, followed by fluorescence reporting by the combination probe QCy-BA $\subset$ Drew-AT. (b) Fluorescence spectra of combination probe QCy-BA $\subset$ Drew-AT in the presence of GOx (4 U/mL) and upon addition of glucose (1 mM). (c) Time-dependent fluorescence of combination probe QCy-BA $\subset$ Drew-AT in the presence and absence of GOx (4 U/mL) upon addition of glucose (1 mM). (d) Photographs of QCy-BA $\subset$ Drew-AT complex under UV-light in the presence of GOx (4 U/mL) with increasing glucose concentration 0.0 to 1.0 mM.

DT in response to H<sub>2</sub>O<sub>2</sub> (100  $\mu$ M) stimulus, in the presence of Drew-AT duplex. The change in fluorescence intensities at 500 nm and 650 nm corresponding to emission maxima ( $E_{max}$ ) of QCy-BA and QCy-DT in the presence of Drew-AT was monitored. Upon excitation at 400 nm, the fluorescence intensity of QCy-BA gradually decreased at 500 nm while that of QCy-DT increased at 650 nm (Fig. 3d). Similarly, the fluorescence spectra recorded upon excitation at 564 nm showed an exponential increase in emission intensity at 650 nm as a function of time and reached saturation  $\geq$  4 h (Fig. S7). The calculation of kinetics parameter using pseudo-first-order conditions for conversion of QCy-BA (2  $\mu$ M) to QCy-DT in the presence of H<sub>2</sub>O<sub>2</sub> (1 mM) and Drew-AT (2  $\mu$ M) gave the rate constant of  $k_{obs} = 1.0 \times 10^{-3} \text{ s}^{-1}$  (Fig. S8).<sup>21</sup> Overall, photophysical

(absorption and emission) studies demonstrated that H<sub>2</sub>O<sub>2</sub> triggers the slicing of phenyl boronic acid functionality of QCy-BA to generate QCy-DT, a DNA minor binding probe that shows switch-on NIR fluorescence in the presence of Drew-AT duplex (Fig. 3e).

**Probing of *in situ* generated H<sub>2</sub>O<sub>2</sub> using combination probe QCy-BA $\subset$ Drew-AT.** In biological systems, enzymes such as oxidases generate H<sub>2</sub>O<sub>2</sub> by the oxidation of numerous biochemicals. Glucose oxidase (GOx) is one of the most important enzymes known to selectively catalyze the oxidation of glucose to gluconic acid in the presence of oxygen, to generate H<sub>2</sub>O<sub>2</sub>. In this context, we set out to probe the *in situ* generation of H<sub>2</sub>O<sub>2</sub> by the oxidation of glucose in the presence of GOx, using our combination probe QCy-BA $\subset$ Drew-AT (Fig. 4a). To monitor the *in situ* generation of H<sub>2</sub>O<sub>2</sub>, glucose was added to PBS buffer (10 mM, pH = 7.4) containing GOx (4 U/mL) and QCy-BA $\subset$ Drew-AT (2  $\mu$ M). The reaction mixture showed a gradual decrease in fluorescence at 500 nm ( $\lambda_{ex} = 400 \text{ nm}$ ) and a corresponding increase in fluorescence intensity at 650 nm (Fig. S9a). Similarly, upon excitation at 564 nm, the fluorescence spectra showed a strong enhancement in fluorescence emission at 650 nm, which may be attributed to the release and binding of QCy-DT to Drew-AT (Fig. 4b). Next, the reaction kinetics of *in situ* generation of H<sub>2</sub>O<sub>2</sub> through the oxidation of glucose by GOx was investigated using the combination probe, upon excitation at 564 nm. The fluorescence intensity at 650 nm was plotted as a function of time, after the addition of glucose (Fig. 4c). Upon addition of glucose (1 mM) in the presence of GOx, QCy-BA $\subset$ Drew-AT showed a gradual increase in fluorescence intensity at 650 nm and reached saturation at 1 h. However, in the absence of glucose, GOx and QCy-BA $\subset$ Drew-AT did not show such increase in fluorescence intensity. Further, the fluorescence was monitored by adding increasing concentrations of glucose (0 to 1 mM) to the mixture of GOx and QCy-BA $\subset$ Drew-AT. The fluorescence emission at 650 nm increases and showed a linear relationship in the concentration range of 0 to 0.2 mM (Fig. 4d and Fig. S9b). Based on  $3\sigma/\text{slope}$ , the LOD of H<sub>2</sub>O<sub>2</sub> was found to be 6.11  $\mu$ M (from the concentration of glucose) and is in good agreement with LOD of H<sub>2</sub>O<sub>2</sub> (5.33  $\mu$ M) using the

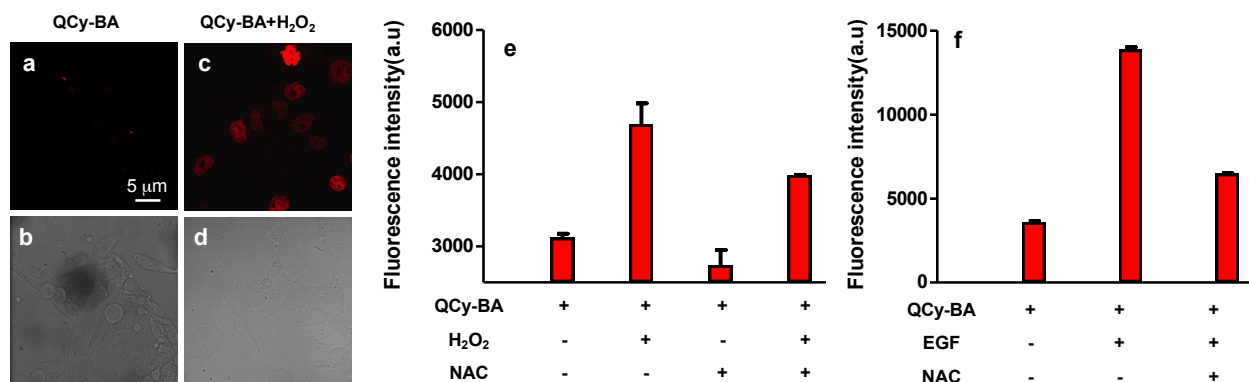


**Fig. 5** (a-b) Fluorescence microscope and differential interference contrast (DIC) images of HeLa cells incubated with QCy-BA (5  $\mu$ M) in the absence of H<sub>2</sub>O<sub>2</sub>. (c-d) Fluorescence microscope and differential interference contrast (DIC) images of HeLa cells incubated with QCy-BA (5  $\mu$ M) in the presence of H<sub>2</sub>O<sub>2</sub> (100  $\mu$ M). Fluorescence images were collected from 600–800 nm upon excitation at 400 nm. (e-f) FACS/flow cytometry analysis shows the PerCP mean fluorescence intensity in HeLa cells. (e) Fluorescence intensity of QCy-BA (5  $\mu$ M) in HeLa cells upon addition of H<sub>2</sub>O<sub>2</sub> (100  $\mu$ M) and N-acetyl-L-cysteine (NAC) (8 mM). (f) Fluorescence intensity of QCy-BA (5  $\mu$ M) in HeLa cells upon addition of epidermal growth factor (EGF) (50 ng/mL) and N-acetyl-L-cysteine (NAC) (8 mM). Error bars represent  $\pm$ standard deviation. PerCP channel:  $\lambda_{ex} = 482 \text{ nm}$  and  $\lambda_{em} = 675 \text{ nm}$ .

combination probe (Fig. S10). From the pseudo-first-order calculations, combination probe **QCy-BA**–Drew-AT (2  $\mu\text{M}$ ) showed the rate constant of  $k_{\text{obs}} = 6.87 \times 10^{-4} \text{ s}^{-1}$  in the presence of GOx (4 U/mL) and glucose (1 mM) (Fig. S11).<sup>21</sup> Overall, GOx assay demonstrated the *in situ* monitoring of  $\text{H}_2\text{O}_2$  generated from the oxidation of glucose.

Next, we studied the effect of an enzyme that spontaneously decomposes  $\text{H}_2\text{O}_2$ , on the conversion of **QCy-BA** to **QCy-DT** by the action of  $\text{H}_2\text{O}_2$ . Catalase is one of the most efficient enzymes that convert  $\text{H}_2\text{O}_2$  to water and oxygen to protect cells from oxidative damage and ROS. Catalase exhibits highest turnover number for  $\text{H}_2\text{O}_2$  and is capable of decomposing almost  $10^6$  molecules per second to water and oxygen. Interestingly, the fluorescence emission was not observed at 650 nm upon addition of  $\text{H}_2\text{O}_2$  (1 mM) to a solution of **QCy-BA**–Drew-AT (2  $\mu\text{M}$ ) containing catalase (4 U/mL). The seized fluorescence emission at 650 nm can be attributed to the prevention of **QCy-BA** to **QCy-DT** conversion, as the added  $\text{H}_2\text{O}_2$  was used as a substrate by the catalase (Fig. S12). These results validate that our combination probe **QCy-BA**–Drew-AT is a promising molecular tool for monitoring the *in situ* turnover of  $\text{H}_2\text{O}_2$  involving oxidase and catalase.

**Fluorescence imaging and cytotoxicity studies of QCy-BA in the presence of  $\text{H}_2\text{O}_2$ .** Remarkable selectivity of **QCy-BA** towards  $\text{H}_2\text{O}_2$  and its detection through DNA-assisted switch-on NIR fluorescence inspired us to evaluate the uptake and application of the probe to detect  $\text{H}_2\text{O}_2$  in cells. For this purpose, confocal fluorescence imaging of HeLa cells treated with  $\text{H}_2\text{O}_2$  (exogenous) was carried out. First, the HeLa cells were incubated with **QCy-BA** (5  $\mu\text{M}$ ) for 30 min and imaged under a confocal microscope. Confocal fluorescence images of these HeLa cells did not show any emission in the red channel (Fig. 5a-b). HeLa cells containing **QCy-BA** were then treated with  $\text{H}_2\text{O}_2$  (100  $\mu\text{M}$ ) for 15 min, after which the cells were again scanned under a confocal microscope. Confocal images of these cells showed strong fluorescence in the red channel with maximum localization in the cell nucleus (Fig. 5c-d). Interestingly, cells also showed the pattern of black nucleoli, a characteristic feature of specific DNA minor groove binders

over single-strand DNA and RNAs.<sup>23</sup> Cell viability assay was performed in HeLa cells to check the cytotoxicity of probe **QCy-BA**. Upon incubation with **QCy-BA**, more than 80% of the cells were viable even at 25  $\mu\text{M}$  concentration after 24 h (Fig. S13). In general, above results confirm the permeability and non-toxicity (at standard working concentration and time of 5  $\mu\text{M}$  and 24 h, respectively) of **QCy-BA**, and detection of exogenously added  $\text{H}_2\text{O}_2$  in HeLa cells through selective fluorescence staining of the cell nucleus.

**Monitoring of *in situ* generated  $\text{H}_2\text{O}_2$  levels by EGF/Nox pathways and post-genotoxic stress in live cells.** NMR, photophysical study, GOx-assay and confocal fluorescence imaging of HeLa cells showed the detection of exogenously added  $\text{H}_2\text{O}_2$  using **QCy-BA**. Next, we employed **QCy-BA** for probing cellular (physiologically generated)  $\text{H}_2\text{O}_2$  levels, in live cells. HeLa cells were incubated with **QCy-BA** (5  $\mu\text{M}$ ) for 30 min in the absence and presence of N-acetyl-L-cysteine (NAC), a well-known  $\text{H}_2\text{O}_2$  scavenger.<sup>24</sup> In the absence of NAC, flow cytometry analysis of cells treated with the probe (5  $\mu\text{M}$ ) showed an increase in mean fluorescence intensity of PerCP as compared to control cells (Fig. S14). Upon addition of NAC (8 mM), the fluorescence intensity of PerCP decreased significantly (Fig. 5e and Fig. S15a). In a control experiment, flow cytometry analysis of live HeLa cells treated with **QCy-BA** and  $\text{H}_2\text{O}_2$  (100  $\mu\text{M}$ ) for 30 min at 37  $^\circ\text{C}$  showed an increase in the mean fluorescence intensity of PerCP (Fig. 5e and Fig. S15a). Thus, probe **QCy-BA** is also capable of detecting the cellular  $\text{H}_2\text{O}_2$  levels in live cells.

Further, our study was extended to visualize the *in situ*  $\text{H}_2\text{O}_2$  generation by a known signaling pathway in live cells. We selected the well-known epidermal growth factor (EGF) binding to epidermal growth factor receptor (EGFR) signaling pathway, which stimulates the production of  $\text{H}_2\text{O}_2$  in cells by activating the NOX/PI3K pathways.<sup>10d</sup> In this experiment, live HeLa cells were incubated with the epidermal growth factor (EGF) (50 ng/mL) for 40 min under physiological conditions (37  $^\circ\text{C}$ , pH = 7.4). EGF-treated live HeLa cells were incubated with **QCy-BA** (5  $\mu\text{M}$ ) for 30 min and flow cytometry analysis of these cells showed strong fluorescence intensity in the PerCP

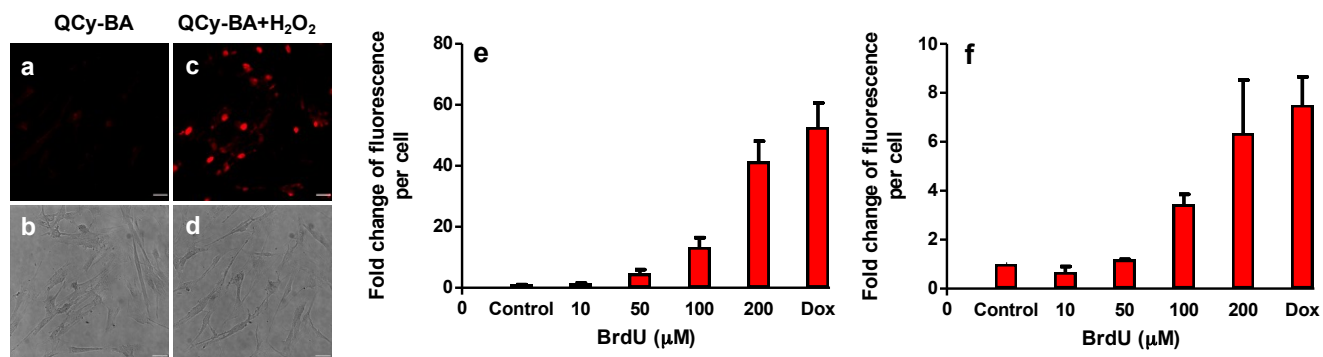


**Fig. 6** (a-b) Fluorescence microscopy and differential interference contrast (DIC) images of MRC5 cells incubated with **QCy-BA** (5  $\mu\text{M}$ ) in the absence of  $\text{H}_2\text{O}_2$ . (c-d) Fluorescence microscope and differential interference contrast (DIC) images of MRC5 cells incubated with **QCy-BA** (5  $\mu\text{M}$ ) in the presence of  $\text{H}_2\text{O}_2$  (100  $\mu\text{M}$ ). Scale bar 5  $\mu\text{m}$ . (e)  $\text{H}_2\text{O}_2$  detection in attached live HeLa cells using **QCy-BA** (5  $\mu\text{M}$ ) after treatment with BrdU from 0 to 200  $\mu\text{M}$  or doxorubicin (0.1  $\mu\text{M}$ ) for 48 h. Fold change of fluorescence per cell is normalized to 1 for control cells (n=3). (f) MRC5 cells were treated with BrdU from 0 to 200  $\mu\text{M}$  or doxorubicin (0.1  $\mu\text{M}$ ) for 72 h.  $\text{H}_2\text{O}_2$  levels were estimated using **QCy-BA** (5  $\mu\text{M}$ ) dye and fold change of fluorescence per cell is normalized to 1 for control cells (n=3).

region (Fig. 5f and Fig. S15b). On the other hand, the control experiment performed on live HeLa cells without EGF stimulation showed modest fluorescence due to the presence of cellular  $\text{H}_2\text{O}_2$  level. In contrast, NAC-treated cells showed a decrease in fluorescence even in the presence of EGF (Fig. 5f and Fig. S15b). FACS-analysis showed 2-fold higher NIR-fluorescence response in cells incubated with EGF (50 ng/mL) compared to cells treated with external  $\text{H}_2\text{O}_2$  (100  $\mu\text{M}$ ). In cells treated with external source of  $\text{H}_2\text{O}_2$ , antioxidants enzymes rapidly consume and decreases its intracellular concentration by  $\sim 7$ -10 folds.<sup>25</sup> Consequently, the relative intracellular concentration of  $\text{H}_2\text{O}_2$  available to react with probe **QCy-BA** is  $\sim 7$ -10 folds lower than the original concentration of externally added  $\text{H}_2\text{O}_2$ . On the other hand, EGF binds to EGFR and induces the production of intracellular  $\text{H}_2\text{O}_2$  in cells. Therefore, concentration of  $\text{H}_2\text{O}_2$  readily available to react with **QCy-BA** is more in case of EGF treated cells, which in turn resulted in higher fluorescence response. These results provided concrete evidence that **QCy-BA** is a versatile and practically viable molecular probe for monitoring concentration levels of  $\text{H}_2\text{O}_2$  in live cells.

In order to detect the *in situ* generated  $\text{H}_2\text{O}_2$  in other physiological conditions, we performed fluorescent plate reader-based studies for cellular senescence in primary and cancer cells using probe **QCy-BA**. First, we performed the fluorescence imaging of primary cells using probe **QCy-BA** in the presence of  $\text{H}_2\text{O}_2$ . Live cell imaging of MRC5 cells showed NIR fluorescence in the nucleus compared to control cells incubated with probe **QCy-BA** (5  $\mu\text{M}$ ) for 30 min after treating with  $\text{H}_2\text{O}_2$  (100  $\mu\text{M}$ ) (Fig. 6a-d). It is well-established that genotoxic stress causes DNA damage in cells that can trigger the generation and accumulation of  $\text{H}_2\text{O}_2$  inside the cells.<sup>26</sup> Recently, it has been shown that DNA damage induced cell cycle arrest or cellular senescence, where ROS played an integral role.<sup>27</sup> To measure ROS generated concomitant to the dose of the DNA damage, HeLa cells were treated with increasing doses (0 to 200  $\mu\text{M}$ ) of 5-bromo-2'-deoxyuridine (BrdU). BrdU is a thymidine analog, which gets directly incorporated into DNA and triggers DNA damage response. From previous studies, we know that 48 h of treatment with BrdU (100  $\mu\text{M}$ ) or another DNA damaging agent, doxorubicin at a concentration of 0.1  $\mu\text{M}$  can lead to the induction of cellular senescence.<sup>7b,27b</sup> After 48 h of treatment with BrdU (100  $\mu\text{M}$ ), HeLa cells showed a 3-fold increase in fluorescence of 2',7'-dichlorofluorescein diacetate (DCFDA) compared to control cells; DCFDA is a known ROS probe for live cells (Fig. S16). Interestingly, probe **QCy-BA** showed an almost 10-fold increase in fluorescence compared to control cells unlike DCFDA, which showed only 3–4 fold change, suggesting that **QCy-BA** dye has a much better dynamic range than DCFDA (Fig. 6e).

Further, similar experiments were performed in primary MRC5 cells, which are human lung primary fibroblasts. To induce DNA damage, MRC5 cells were similarly treated with various doses of BrdU and doxorubicin (0.1  $\mu\text{M}$ ) for 72 h. After 72 h, probe **QCy-BA** showed increase in fluorescence compared to control cells in a dose-dependent manner,

indicating that the probe can be used to monitor the *in situ* generated  $\text{H}_2\text{O}_2$  in primary cells as well (Fig. 6f). Therefore, above results reveal that **QCy-BA** is a versatile probe to monitor the elevated levels of  $\text{H}_2\text{O}_2$  in both primary and cancer cells in the senescence state.

## Conclusions

In conclusion, we developed a stimuli-responsive, colorimetric and switch-on NIR fluorescence combination probe (**QCy-BA** in combination with AT-rich exogenous or endogenous nuclear DNA) for  $\text{H}_2\text{O}_2$ . In **QCy-BA**, the phenyl boronic acid functionality effectively suppressed the NIR fluorescence of **QCy-DT**, a DNA minor groove binder and restored selectively in the presence of  $\text{H}_2\text{O}_2$ . NMR and UV-vis absorption study showed selective conversion of **QCy-BA** to **QCy-DT** and quinine methide in response to  $\text{H}_2\text{O}_2$  while the solution color changed from yellow to brown for naked eye detection of  $\text{H}_2\text{O}_2$  over other ROS. The fluorescence study demonstrated selective conversion of **QCy-BA** to **QCy-DT** in response to  $\text{H}_2\text{O}_2$  stimulus that showed NIR fluorescence in the presence of AT-rich DNA duplex (Drew-AT). Further, glucose oxidase assay confirmed the use of combination probe **QCy-BA** < DNA for probing *in situ* generated  $\text{H}_2\text{O}_2$  by the oxidation of glucose to gluconic acid. Cell viability and confocal fluorescence imaging of HeLa cells showed the cell permeability, non-toxicity and preferential nuclear staining of the probe in the presence of  $\text{H}_2\text{O}_2$ . Furthermore, **QCy-BA** is a sensitive probe to detect normal and *in situ* generated levels of  $\text{H}_2\text{O}_2$  by EGF/Nox pathways in live cells. Probe **QCy-BA** was also found to be effective in the detection of  $\text{H}_2\text{O}_2$  in the primary cells as well as senescent cancer cells. Therefore, ease of synthesis, large Stokes shift, cell permeability and ability to detect normal and elevated levels of  $\text{H}_2\text{O}_2$  in primary as well as cancer cells makes **QCy-BA** a superior combination probe with NIR fluorescence response (Table S1). We anticipate that our approach of conjugating DNA fluorescence probes with stimuli-responsive appendages (combination probes) will open up new avenues in the development of DNA targeting theranostic prodrugs for targeting disease-associated cells. This approach can be further extended to create new stimuli-responsive probes for various biochemical processes including enzymatic activities.

## Experimental Section

**General information.** All the chemicals, reagents, self-complementary Drew-AT, Hoechst 33258, Phosphate buffer saline (PBS), 2',7'-dichlorofluorescein (DCFDA), 5-bromo-2'-deoxyuridine (BrdU), doxorubicin (dox), Hydrogen peroxide ( $\text{H}_2\text{O}_2$ ), tertbutylhydroperoxide (TBHP), potassium superoxide ( $\text{KO}_2$ ), Sodium hypochlorite (NaOCl), Diethylamine NONOate sodium salt hydrate, Sodium nitrite ( $\text{NaNO}_2$ ) and N-acetyl-L-cysteine (NAC) were purchased from Sigma-Aldrich. All synthesized compounds were purified by column chromatography using Rankem silica gel (60-120 mesh). <sup>1</sup>H and



$^{13}\text{C}$  NMR spectra were recorded on a Bruker AV-400 MHz spectrometer with chemical shifts reported as parts per million (*ppm*) (in  $\text{CDCl}_3$ ,  $\text{DMSO-}d_6$ , tetramethylsilane as an internal standard) at 20 °C. High resolution mass spectra (HRMS) were obtained on Agilent Technologies 6538 UHD Accurate-Mass Q-TOF LC/MS spectrometer. The UV-vis absorption and emission spectra were recorded on Agilent Technologies Cary series UV-vis-NIR absorbance and Cary Eclipse fluorescence spectrophotometers, respectively. UV-vis absorption and emission spectra were measured in quartz cuvettes of 1 cm path length.

**Sample preparation for UV-vis and fluorescence measurements.** A stock solution of probe **QCy-BA** was prepared in millimolar concentration in Milli-Q water (MQ-water) and stored at -10 °C. DNA stock solutions were prepared by dissolving oligos in double-distilled water in the order of  $10^{-4}$  M. Double-stranded DNA samples were prepared in PBS (10 mM, pH = 7.4) buffer solution and subjected to annealing by heating up to 85 °C for 15 min, followed by subsequent cooling to room temperature for 7 h and storing in a refrigerator for 4 h.<sup>16d</sup> Peroxynitrite (ONOO<sup>-</sup>) solution was prepared according reported literature.<sup>28</sup>

**Maintenance of HeLa cells.** Human cervix carcinoma cell line (HeLa) was cultured in DMEM (Dulbecco's Modified Eagle's Medium) with 10 % FBS (Fetal Bovine Serum). The antibiotics penicillin and streptomycin (1 %) were mixed with 10 % FBS medium. The cells were incubated at 37 °C temperature in a 5 %  $\text{CO}_2$  humidified chamber. All cell culture work was carried out under laminar flow hood.

**Cytotoxicity studies on HeLa cells (MTT assay).** MTT [(3-(4,5-dimethylthiazol-2yl)-2,5-diphenyltetrazolium bromide)] assay was carried out with probe **QCy-BA** on HeLa cells to determine the cytotoxicity effect. In a tissue culture 96-well plate, 10,000 cells per well were plated and grown for 24 h. Cells were treated with various concentrations (25  $\mu\text{M}$ , 12.5  $\mu\text{M}$ , 6.25  $\mu\text{M}$ , 3.125  $\mu\text{M}$  and 0  $\mu\text{M}$ ) of probe **QCy-BA** for 24 h. All the treatments were carried out in triplicates. The required concentrations of **QCy-BA** were made from a 1mg/ml aqueous stock solution in 0.2% DMEM. Four hours before stipulated time of the experiment, MTT-solution (5 mg/mL of 20  $\mu\text{L}$ ) was added to each well and incubated to form formazan crystals. The culture medium was completely removed by a 1 mL pipette, and 200  $\mu\text{L}$  of DMSO was added to dissolve the formazan crystals. The purple-colored formazan was estimated by determining absorbance at 590 nm with the help of a spectrophotometer (Bio-RAD model 1680, Microplate reader). The results were represented as bar graphs (Concentration of **QCy-BA** vs. % Cell viability).

**Exogenous and endogenous detection of  $\text{H}_2\text{O}_2$  in HeLa cells by **QCy-BA**.** For the detection of endogenous  $\text{H}_2\text{O}_2$  in HeLa cells by flow cytometric analysis,  $3 \times 10^5$  HeLa cells were plated in each well of 6-well tissue culture plates and grown for 24 h. Cells were serum deprived for 1 h. In addition, the serum-deprived cells of the 6-well tissue culture plates were treated with N-acetyl-L-cysteine (NAC) (8 mM) and incubated for 1 h. Post this, cells were treated with the probe **QCy-BA** (5  $\mu\text{M}$ ) and incubated for 30 min. After 30 min incubation, the cells were

washed with DPBS (Dulbecco's Phosphate buffer saline) to remove the excess of **QCy-BA**. These cells were harvested after trypsinization. Exogenously,  $\text{H}_2\text{O}_2$  (100  $\mu\text{M}$ ) was added to **QCy-BA** and NAC+**QCy-BA** treated cells and incubated for 15 min. These samples were subjected to FACS analysis in the PerCP ( $\lambda_{\text{ex}} = 482$  nm and  $\lambda_{\text{em}} = 675$  nm) channel.

**Epidermal growth factor (EGF)-generated  $\text{H}_2\text{O}_2$  detection by **QCy-BA** in HeLa cells.** In a 12-well plate,  $3 \times 10^5$  HeLa cells were plated in each well and grown for 24 h. Cells were serum-deprived for 1h. Three wells of serum-deprived cells were treated with NAC (8 mM) for 1 h. Then cells were treated with **QCy-BA** (5  $\mu\text{M}$ ) for 30 min. After 30 min incubation of cells with **QCy-BA**, cells were washed with DPBS (Dulbecco's Phosphate Buffer Saline) to remove the excess of **QCy-BA**. The cells were harvested after trypsinization and a single cell suspension was made. The distribution of **QCy-BA**-stained HeLa cells were determined by flow cytometry in the PerCP channel.

**Immunofluorescence studies with **QCy-BA** for detection of  $\text{H}_2\text{O}_2$  in HeLa cells.** Immunofluorescence studies were carried out in HeLa cells to validate exogenous and endogenous detection of  $\text{H}_2\text{O}_2$  by **QCy-BA**. The HeLa cells (10,000 cells) were grown on cover slips. These cells were treated with 5  $\mu\text{M}$  concentration of **QCy-BA** for 30 min. The cells were washed several times with DPBS to remove the excess of **QCy-BA**. The cells were treated with  $\text{H}_2\text{O}_2$  (100  $\mu\text{M}$ ) for 30 min. These samples were subjected to confocal microscopy for immunofluorescence images and images were collected from 600–800 nm upon excitation at 400 nm. Fluorescence images were taken by Carl Zeiss Laser Scanning Microscope (LSM510 META).

**Detection of ROS using fluorescence plate reader.** The cells were incubated with **QCy-BA** (5  $\mu\text{M}$ ) for 30 min in dark, washed with PBS and analyzed to detect **QCy-BA** dye fluorescence using Infinite M1000 Pro, Tecan, Austria. Wavelengths used for excitation and emission for **QCy-BA** dye was 400nm/650nm. The ROS measurement assays were conducted using plate reader and after fluorescence measurements, cells were washed, trypsinized and counted to estimate fluorescence per cell recordings.

**Live cell imaging of MRC5 cells.** MRC5 PDL 23 cells were seeded overnight and treated with  $\text{H}_2\text{O}_2$  for live cell imaging after the addition of **QCy-BA** (5  $\mu\text{M}$ ) for 30 min. Images were acquired using Olympus IX 83 inverted epifluorescence microscope using a 20X objective from 600–800 nm upon excitation at 400 nm.

## Acknowledgements

We thank Prof. C. N. R. Rao FRS for constant support and encouragement, the Council of Scientific and Industrial Research (CSIR) New Delhi, [grant No. 02/(0128)/13/EMR-II], Innovative Young Biotechnologist Award (IYBA) and the Department of Biotechnology (DBT), India (BT/03/IYBA/2010) for financial support, Alexander von Humboldt Foundation, Germany for special equipment donation to T.G, ICMS-JNCASR

for awarding Sheikh Saqr Career Award Fellowship to T.G. CSIR for SRF fellowship to N.N.

## Notes and references

- (a) C. C. Winterbourn, *Nat. Chem. Biol.*, 2008, **4**, 278–286; (b) P. D. Ray, B.-W. Huang, and Y. Tsuji, *Cell. Signal.*, 2012, **24**, 981–990.
- (a) R. A. Cairns, I. S. Harris and T. W. Mak, *Nat. Rev. Cancer*, 2011, **11**, 85–95; (b) C. Gorrini, I. S. Harris and T. W. Mak, *Nat. Rev. Drug Discov.*, 2013, **12**, 931–947.
- (a) T. P. Szatrowski and C. F. Nathan, *Cancer Res.*, 1991, **51**, 794–798; (b) S. Toyokuni, K. Okamoto, J. Yodoi and H. Hiai, *FEBS Lett.*, 1995, **358**, 1–3; (c) K. P. Mishra, *J. Environ. Pathol. Toxicol. Oncol.*, 2004, **23**, 61–66; (d) S. Kawanishi, Y. Hiraku, S. Pinlaor and N. Ma, *Biol. Chem.*, 2006, **387**, 365–372.
- (a) F. Q. Schafer and G. R. Buettner, *Free Radic. Biol. Med.*, 2001, **30**, 1191–1212; (b) J. Boonstra and J. A. Post, *Gene*, 2004, **337**, 1–13; (c) M. P. Murphy, A. Holmgren, N.-G. Larsson, B. Halliwell, C. J. Chang, B. Kalyanaraman, S. G. Rhee, P. J. Thornalley, D. Gems, T. Nyström, V. Belousov, P. T. Schumacker and C. C. Winterbourn, *Cell Metab.*, 2011, **13**, 361–366.
- (a) G. Perry, K. A. Raine, A. Nunomura, T. Watayc, L. M. Sayre and M. A. Smith, *Free Radic. Biol. Med.*, 2000, **28**, 831–834; (b) B. Halliwell and J. M. C. Gutteridge, *Free Radicals in Biology and Medicine* 1–677, Oxford University Press, Oxford, 2007.
- (a) M. T. Lin and M. F. Beal, *Nature*, 2006, **443**, 787–795; (b) N. Houstis, E. D. Rosen and E. S. Lander, *Nature*, 2006, **440**, 944–948; (c) D. Jay, H. Hitomi and K. K. Griendling, *Free Radic. Biol. Med.*, 2006, **40**, 183–192; (d) J. P. Fruehauf and F. L. Jr. Meysken, *Clin. Cancer Res.*, 2007, **13**, 789–794. (e) T. Finkel, M. Serrano and M. A. Blasco, *Nature*, 2007, **448**, 767–774. (f) D. Trachootham, J. Alexandre and P. Huang, *Nat. Rev. Drug Discov.*, 2009, **8**, 579–591.
- (a) R. Colavitti and T. Finkel, *IUBMB Life*, 2005, **57**, 277–281. (b) R. R. Nair, M. Bagheri and D. K. Saini, *J. Cell. Sci.*, 2015, **128**, 342–353.
- (a) B. Chance, H. Sies and A. Boveris, *Physiol. Rev.*, 1979, **59**, 527–605; (b) M. Lopez-Lazaro, *Cancer Lett.*, 2007, **252**, 1–8.
- S. G. Rhee, *Science*, 2006, **312**, 1882–1883.
- (a) K. N. Schmidt, P. Amstad, P. Cerutti and P. A. Baeuerle, *Chem. Biol.*, 1995, **2**, 13–22; (b) M. Sundaresan, Z. X. Yu, V. J. Ferrans, K. Irani and T. Finkel, *Science*, 1995, **270**, 296–299; (c) K. Z. Guyton, Y. Liu, M. Gorospe, Q. Xu and N. J. Holbrook, *J. Biol. Chem.*, 1996, **271**, 4138–4142; (d) Y. S. Bae, S. W. Kang, M. S. Seo, I. C. Baines, E. Tekle, P. B. Chock and S. G. Rhee, *J. Biol. Chem.*, 1997, **272**, 217–221; (e) S. R. Lee, K. S. Kwon, S. R. Kim and S. G. Rhee, *J. Biol. Chem.*, 1998, **273**, 15366–15372; (f) M. V. Avshalumov and M. E. Rice, *Proc. Natl. Acad. Sci. USA*, 2003, **100**, 11729–11734; (g) Z. A. Wood, L. B. Poole and P. A. Karplus, *Science*, 2003, **300**, 650–653.
- (a) E. W. Miller, A. E. Albers, A. Pralle, E. Y. Isacoff and C. J. Chang, *J. Am. Chem. Soc.*, 2005, **127**, 16652–16659; (b) D. Lee, S. Khaja, J. C. Velasquez-Castano, M. Dasari, C. Sun, J. Petros, W. R. Taylor and N. Murthy, *Nat. Mater.*, 2007, **6**, 765–769; (c) A. E. Albers, B. C. Dickinson, E. W. Miller and C. J. Chang, *Bioorg. Med. Chem. Lett.*, 2008, **18**, 5948–5950; (d) B. C. Dickinson, Y. Tang, Z. Chang and C. J. Chang, *Chem. Biol.*, 2011, **18**, 943–948; (e) A. R. Lippert, G. C. Van de Bittner and C. J. Chang, *Acc. Chem. Res.*, 2011, **44**, 793–804; (f) J. Chan, S. C. Dodani and C. J. Chang, *Nature Chem.*, 2012, **4**, 973–984. (g) Y. Wen, K. Liu, H. Yang, Y. Li, H. Lan, Y. Liu, X. Zhang and T. Yi, *Anal. Chem.*, 2014, **86**, 9970–9976.
- (a) E. W. Miller, O. Tulyathan, E. Y. Isacoff and C. J. Chang, *Nat. Chem. Biol.*, 2007, **3**, 263–267; (b) G. C. Van de Bittner, C. R. Bertozzi and C. J. Chang, *J. Am. Chem. Soc.*, 2013, **135**, 1783–1795; (c) R. Weinstein, E. N. Savariar, C. N. Felsen and R. Y. Tsien, *J. Am. Chem. Soc.*, 2014, **136**, 874–877.
- (a) F. B. Yu, P. Li, P. Song, B. S. Wang, J. Z. Zhao and K. Han, *Chem. Commun.*, 2012, **48**, 4980–4982; (b) Z. Lou, P. Li, X. Sun, S. Yang, B. Wang and K. Han, *Chem. Commun.*, 2013, **49**, 391–393; (c) Z. Lou, P. Li and K. Han, *Acc. Chem. Res.*, 2015, **48**, 1358–1368.
- (a) A. M. Caamaño, M. E. Vázquez, J. Martínez-Costas, L. Castedo and J. L. Mascareñas, *Angew. Chem., Int. Ed.*, 2000, **39**, 3104–3107; (b) J. Rautio, H. Kumpulainen, T. Heimbach, R. Oliyai, D. Oh, T. Järvinen and J. Savolainen, *Nat. Rev. Drug Discov.*, 2008, **7**, 255–270; (c) H. M. Lee, D. R. Larson and D. S. Lawrence, *ACS Chem. Biol.*, 2009, **4**, 409–427; (d) A. Deiters, *ChemBioChem*, 2010, **11**, 47–53.
- (a) M. I. Sanchez, J. M. Costas, F. Gonzalez, M. A. Bermudez, M. E. Vazquez and J. L. Mascareñas, *ACS Chem. Biol.*, 2012, **7**, 1276–1280; (b) P. Murat, M. V. Gormally, D. Sanders, M. D. Antonio and S. Balasubramanian, *Chem. Commun.*, 2013, **49**, 8453–8455; (c) M. I. Sanchez, C. Penas, M. E. Vazquez and J. L. Mascareñas, *Chem. Sci.*, 2014, **5**, 1901–1907; (d) Q. Hu, M. Gao, G. Feng and B. Liu, *Angew. Chem., Int. Ed.*, 2014, **53**, 14225–14229; (e) R. Kumar, J. Han, H. J. Lim, W. X. Ren, J. Y. Lim, J. H. Kim and J. S. Kim, *J. Am. Chem. Soc.*, 2014, **136**, 17836–17843; (f) E.-J. Kim, S. Bhuniya, H. Lee, H. M. Kim, C. Cheong, S. Maiti, K. S. Hong and J. S. Kim, *J. Am. Chem. Soc.*, 2014, **136**, 13888–13894.
- (a) D. Maity, A. Raj, D. Karthigeyan, T. K. Kundu and T. Govindaraju, *RSC Adv.*, 2013, **3**, 16788–16794; (b) D. Maity and T. Govindaraju, *Org. Biomol. Chem.*, 2013, **11**, 2098–2104; (c) D. Maity, A. Raj, P. K. Samanta, D. Karthigeyan, T. K. Kundu, S. K. Pati and T. Govindaraju, *RSC Adv.*, 2014, **4**, 11147–11151; (d) N. Narayanaswamy, M. Kumar, S. Das, R. Sharma, P. K. Samanta, S. K. Pati, S. K. Dhar, T. K. Kundu and T. Govindaraju, *Sci. Rep.*, 2014, **4**, 6476.
- N. Narayanaswamy, S. Das, P. K. Samanta, K. Banu, G. P. Sharma, N. Mondal, S. K. Dhar, S. K. Pati and T. Govindaraju, *Nucleic Acids Res.*, 2015, **43**, 8651–8663.
- H. G. Kuivila and A. G. Armour, *J. Am. Chem. Soc.*, 1957, **79**, 5659–5662.
- R. B. Greenwald, A. Pendri, C. D. Conover, H. Zhao, Y. H. Choe, A. Martinez, K. Shum and S. Guan, *J. Med. Chem.*, 1999, **42**, 3657–3667.
- (a) N. Karton-Lifshin, E. Segal, L. Omer, M. Portnoy, R. Satchi-Fainaro and D. Shabat, *J. Am. Chem. Soc.*, 2011, **133**, 10960–10965; (b) S. Gnaïm and D. Shabat, *Acc. Chem. Res.*, 2014, **47**, 2970–2984.
- C. Chang, D. Srikan, C. S. Lim, C. J. Chang and B. R. Cho, *Chem. Commun.*, 2011, **47**, 9618–9620.
- (a) M. Coll, C. A. Frederick, A. H. J. Wang and A. Rich, *Proc. Natl. Acad. Sci. USA*, 1987, **84**, 8385–8389; (b) N. Spink, D. G. Brown, J. V. Skelly and S. Neidle, *Nucleic Acids Res.*, 1994, **22**, 1607–1612.
- G. M. Spitzer, J. E. Fuchs, P. Markt, J. Kirchmair, B. Wellenzohn, T. Langer and K. R. Liedl, *Chemphyschem*, 2008, **9**, 2766–2771.
- C. C. Winterbourn and D. Metodiewa, *Free Radic. Biol. Med.*, 1999, **27**, 322–328.
- (a) F. Antunes and E. Cadenas, *FEBS Lett.* 2000, **475**, 121–126; (b) B. K. Huang and H. D. Sikes, *Redox Biol.*, 2014, **2**, 955–962.
- M. S. Cooke, M. D. Evans, M. Dizdaroglu and J. Lunec, *FASEB J.*, 2003, **17**, 1195–1214.
- (a) F. d'Adda di Fagagna, *Nat. Rev. Cancer.*, 2008, **8**, 512–522; (b) K. M. Tewey, T. C. Rowe, L. Yang, B. D. Halligan and L. F. Liu, *Science*, 1984, **226**, 466–468.
- J. W. Reed, H. H. Ho, W. L. Jolly, *J. Am. Chem. Soc.*, 1974, **96**, 1248–1249.

## Graphical Abstract

### Stimuli-responsive colorimetric and NIR fluorescence combination probe for selective reporting of cellular hydrogen peroxide

N. Narayanaswamy, S. Narra, R. R. Nair, D. K. Saini, P. Kondaiah and T. Govindaraju\*

Stimuli-responsive and NIR fluorescence combination probe (**QCy-BA**⊂DNA) efficiently quantify and image normal and elevated levels of hydrogen peroxide in primary and disease-associated cells.

